Electrochimica Acta 53 (2008) 5174–5179

Contents lists available at ScienceDirect

Electrochimica Acta

journal homepage: www.elsevier.com/locate/electacta

Continuous thin gold films electroless deposited on fibrous mats of polyacrylonitrile and their electrocatalytic activity towards the oxidation of methanol

Bin Guo, Shizhen Zhao, Gaoyi Han*, Liwei Zhang

Institute of Molecular Science, Key Laboratory of Chemical Biology and Molecular Engineering of Education Ministry, Shanxi University, Taiyuan 030006, PR China

ARTICLE INFO

Article history:
Received 6 February 2008
Accepted 16 February 2008
Available online 23 February 2008

Keywords:
Electrospinning
Polyacrylonitrile
Gold
Methanol
Electro-oxidation

ABSTRACT

Polyacrylonitrile nanofibers containing different amounts of gold nanoparticles have been prepared by electrospinning technique. By using the gold nanoparticles as seeds, thin continuous gold films have been deposited on the surface of polyacrylonitrile fibers through self-catalyzed reduction of chloroauric acid in solution. The conductivities of the fibrous mats increase with the amount of gold deposited on the fibers increase. The smooth continuous thin gold films tend to form on the fibers surface when the organic fibers contain more gold seeds, while coarse films tended to form on the fibers containing less gold seeds. The electrocatalytic activity of the fibrous mats electrodes towards the methanol oxidation in alkaline medium has been investigated, indicating that these electrodes exhibit higher electrocatalytic activity than pure gold electrode because of their three-dimensional structures. The results also indicate that the mats with smooth gold coating exhibit higher electrocatalytic activity than that with coarse gold coating.

1. Introduction

Nanomaterials have stimulated great interest in many areas such as catalysis, biological and chemical sensor, and nanotechnology [1–9]. Self-assembly of colloidal metal particles is a powerful method for fabricating macroscopic surfaces with well-defined and controllable nanostructures [10,11]. Recently, they have been applied as substrates for surface plasmon resonance and surface-enhanced Raman spectroscopy, microscale and nanoscale metal patterns in metallic structures [12–15]. The methods for preparing metal films on substrate include chemical vapor deposition, electrodeposition and electroless plating methods, etc. The electroless plating technique is very convenient among these methods. Up to date, gold particles have been successfully deposited on the substrates such as glass, silicon, oxides and organic polymer [16–19] by using electroless plating method.

In the past years, electrospinning technique has been recognized as an efficient method to manufacture nanoscale fibrous structures. Recently, organic [20–24], inorganic [25–27] and organic–inorganic hybrid [28,29] nanofibers with large surface area-to-volume ratio and uniform in diameter have been fabricated because of their potential applications in membrane technology, tissue engineering, optical sensors, biosensors, and drug delivery [20–29]. Furthermore, microfibers or microtubes of metals such as gold, copper, silver and aluminum have been fabricated by using electrospun fibrous mats as template [30–33].

Although bulk gold is a poor catalyst, recent studies show that the gold nanoparticles (GNPs) loaded on the substrates such as carbon [34–37] or other matrix [38–41] exhibit high catalytic activities for CO, methanol and hydrocarbons oxidation in both heterogeneous and homogeneous catalysis [34–41]. According to our knowledge, continuous thin gold layers deposited on electrospun fibers have not been used as electrode for catalysis.

In this paper, nanofibers of polyacrylonitrile (PAN) containing different amounts of GNPs have been prepared through electrospinning technique. And then the continuous thin gold films are deposited on the fibers surface by reducing the chloroauric acid with hydroxylamine in aqueous solution [16,30]. The metallized fibrous mats of PAN can be directly used as electrodes because of their high stability, conductivities and surface area. The electrocatalytic activities of the fibrous mat electrodes towards methanol oxidation have been investigated.

2. Experimental

2.1. Preparation of the hybrid fibers of PAN and gold salt

The chemicals of chloroauric acid, oxammonium hydrochloride and tetrabutyl-ammonium bromide (TBAB) were purchased from Beijing Chemical Company. PAN and sodium borohydride were

* Corresponding author. Tel.: +86 351 7010699; fax: +86 351 7016358.
E-mail address: han_gaoyis@sxu.edu.cn (G. Han).

0013-4686/$ – see front matter © 2008 Elsevier Ltd. All rights reserved.
doi:10.1016/j.electacta.2008.02.060

purchased from Aldrich Company. The gold salt was synthesized by using chloroauric acid and TBAB according to previous method [30], and other chemicals were reagent grade and used directly.

In the typical process, PAN (90 mg) was dissolved in dimethylformamide (1.0 ml) at 80 °C to form a transparent solution, and then different amounts of gold salt (3 mg or 30 mg) were added to the mixture to form a brown-red solution, the concentration of gold salt was 3.2% and 25% (w/w). After the solution had been shaken for about 1 h, the mixture of gold salt and PAN was transferred into a plastic pipette with the inner diameter of ~1 mm. A thin platinum rod was put into the plastic pipette, which was connected to a high-voltage power supply. The potential for electrospinning was kept at +13.7 kV, and the resulted fibers were collected on a filter paper placed upon the grounded aluminum foil, which was 12 cm below the plastic pipette tip.

2.2. Preparation of gold-coated fibrous mats

All glassware was soaked in a mixture of nitric acid (45 ml) and hydrochloric acid (135 ml) for 1 h, and then thoroughly washed with deionized water. The fibrous mats together with the filter paper were cut into disks with a diameter of about 4.0 cm. Then the mats were placed in a vacuum funnel, and dilute $NaBH_4$ solution (1 mmol l^{-1}, 200 ml) was filtered through the mats. After this procedure, the gold salt embedded in PAN fibers was reduced to form GNPs. Then the mats were washed with water (600 ml) and dilute HCl solution (0.1 mol l^{-1}, 400 ml) through filtration. The gold particles immobilized on the polymer surface grew up by filtering electroless plating solution containing 0.1 mg ml^{-1} $HAuCl_4 \cdot 3H_2O$ + 0.02 mg ml^{-1} $NH_2OH \cdot HCl$ until the filtrate became colorless. The metallized mats prepared by filtering 200 ml and 600 ml plating solution were defined as 3S1 and 3S2 for the fibrous mats containing 3.2% gold salt, and 25S1 and 25S2 for containing 25% gold salt.

2.3. Samples characterization

UV–visible spectra were carried out on a Hewlett Packard 8453E single beam diode array recording spectrophotometer. Briefly speaking, a quartz slide coated with the hybrid fibrous mats was placed into the sample holder for measurement. In order to diminish the effect of scattering, a little of DMF was dipped onto the mats. XRD patterns were measured by using a Bruker D8 Advance X-ray diffractometer. A piece of mats was placed on the sample holder and was scanned from 10° to 80° (2θ) at the speed of 0.02°/s. Scanning electron microscopy images were taken by using a (LEO438VP, England) microscope operated at an accelerating voltage of 15 kV. For the measurement of transmission electron microscope (H-600-2, HITACHI, Japan), a piece of PAN/GNPs fibrous mat was placed on a copper grid. The direct current conductivity was measured by conventional four-probe method.

The electrochemical investigations were performed on one-compartment electrolyte cell by using an electrochemical instrument (CHI 660B) under computer control. The metallized fibrous mats with a thickness of ~10 μm were cut into small strips with length of 1.5 cm and width of 0.2 cm, which were clamped by a clamp and used as working electrode, the geometric surfaces of the mats electrodes immerged in electrolyte solution were measured about 0.04 cm^2. A platinum sheet was used as the counter electrode, and a saturated calomel electrode (SCE) was employed as the reference electrode in all electrochemical experiments. The typical electrolyte solution was 0.1 mol l^{-1} KOH or 0.1 mol l^{-1} KOH and CH_3OH aqueous solution. Prior to the electrochemical measurements, high purity argon was used for deaeration of the solutions for 5 min, and during measurements an argon flow was maintained above the electrolyte solution.

3. Results and discussion

3.1. The characterization of gold films deposited on the PAN fibers surface

Fig. 1A shows the TEM images of PAN/GNPs composite fibers prepared from PAN/gold salt fibers, in which the concentration of gold salt is about 3.2% (w/w, the amount of PAN is 90 mg and gold salt is 3 mg). We can find from Fig. 1A that the diameters of the hybrid fibers are 50–200 nm, and the GNPs with diameters of ~5 nm are dispersed separately on the PAN fibers surface and inside because of the low concentration of gold salt. However, the PAN/GNPs hybrid fibers prepared from PAN/gold salt fibers containing 25% gold salt (w/w, the amount of PAN is 90 mg and gold salt is 30 mg) exhibit the diameters ranging from ~150 nm to ~300 nm (Fig. 1B). The GNPs with a diameter of about 10–20 nm are observed in the fibers, and some GNPs aggregate into clusters with a size of ~50 nm. The absorption peak at about 394 nm (Fig. 1C(a)) results from the gold salt embedded in hybrid fibers. When the gold salt embedded in fibers is treated with $NaBH_4$, the color of the fibrous mats turns from yellow to light brown, and the absorption peaks located at about 526 (Fig. 1C(b)) and 540 nm (Fig. 1C(c)) are assigned to the plasmon band of GNPs embedded in PAN/GNPs fibers, prepared from PAN/gold salt fibers containing 3.2% and 25% gold salt, respec-

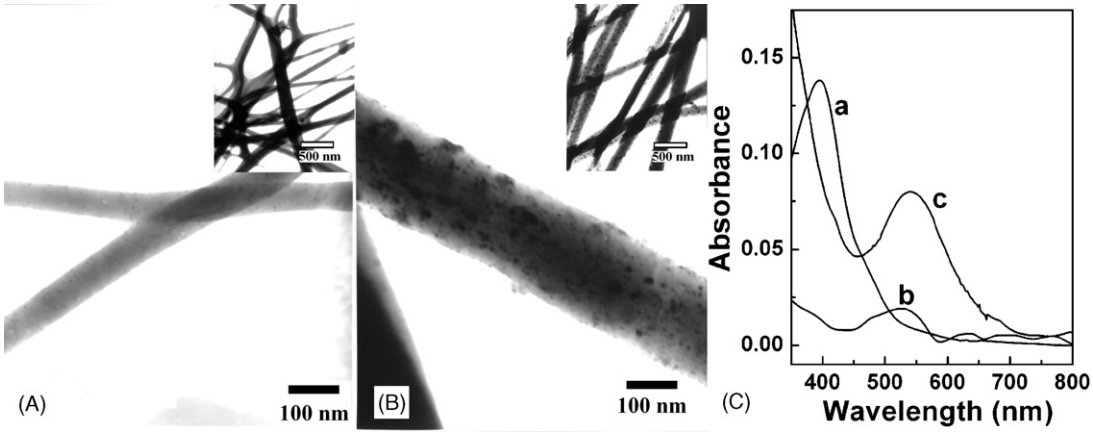

Fig. 1. The TEM images of the hybrid fibers of PAN/GNPs prepared from PAN/gold salt hybrid fibers containing (A) 3.2% and (B) 25% (w/w) gold salt, and (C) the absorption spectra of the hybrid fibers of (a) PAN/gold salt, PAN/GNPs hybrid fibers prepared from PAN/gold salt hybrid fibers containing (b) 3.2% and (c) 25% (w/w) gold salt.

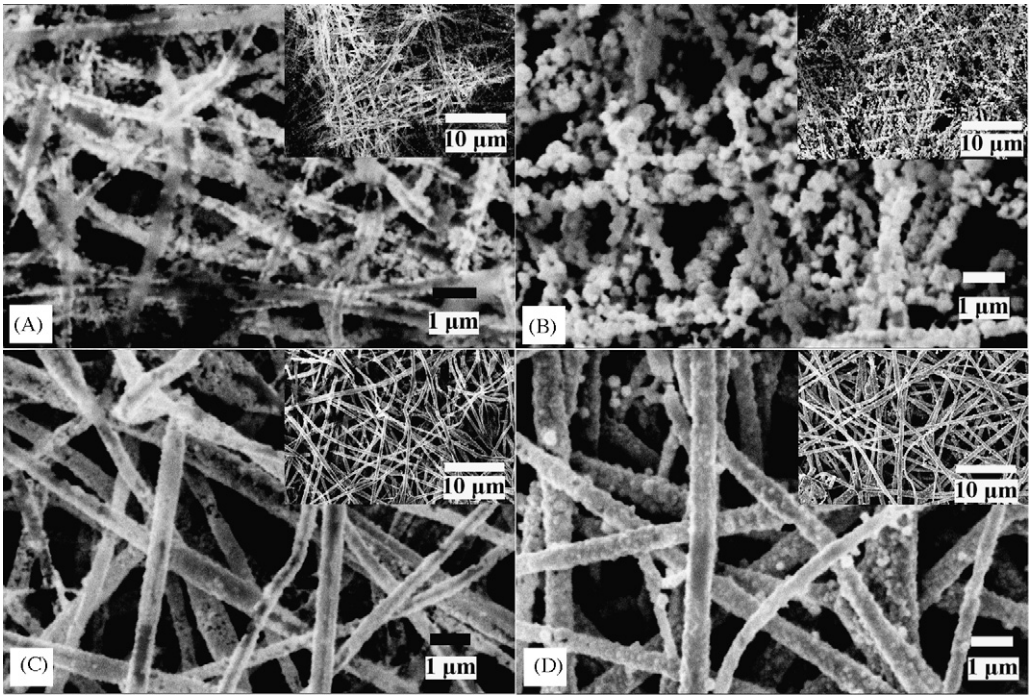

Fig. 2. The SEM micrographs of S1 (treated with 200 ml plating solution) and S3 (treated with 600 ml plating solution): (A) 3S1, (B) 3S2, (C) 25S1 and (D) 25S2.

tively. According to the literatures [16,17], the optical spectra of spherical gold particles with average size of 3.4 nm or larger are generally dominated by the plasmon band centered at around 520 nm. When there is some aggregation between the GNPs, the plasmon band of GNPs shifts to longer wavelengths. The absorption peak located at 540 nm (Fig. 1C(c)) indicates that some aggregation occurs between GNPs, the result is consistent with that of TEM.

Fig. 2 shows the SEM micrographs of the fibrous mats treated with 200 ml and 600 ml plating solution. When the PAN/GNPs fibers (3.2%) are treated with 200 ml plating solution, the sample of 3S1 is obtained. From Fig. 2A, we can find that the gold particles with the diameters of 50–100 nm are roughly spherical in shape and dispersed on the surface of PAN fibers, and the continuous gold films are not formed in 3S1. After more plating solution (600 ml) is used to plate the PAN/GNPs fibers (3.2%), the PAN fibers in 3S2 are covered by the coarse gold films, which are formed by the gold particles with irregular shape and the size of 300–500 nm (Fig. 2B). However, when the PAN/GNPs (25%) hybrid fibrous mats are treated with 200 ml plating solution, the surface of the fibers in 25S1 are covered by almost continuous thin gold films, which are formed by the GNPs with the diameter of ~50 nm (Fig. 2C), when 600 ml plating solution is used to plate the PAN/GNPs (25%) fibrous mats, the fibers in 25S2 are covered by the continuous compact gold films formed by GNPs with the diameters of 100–200 nm (Fig. 2D). In contrast with 3S2, the spherical shape of the GNPs is still retained in 25S2. The reason may be that, the less the gold salt in the PAN/gold salt hybrid fibers, the less the GNPs (gold seeds) formed in the hybrid fibers. Then the reaction between Au^{3+} and NH_2OH can only occur on the less gold seeds, so the grown gold particles are dispersed on the fibers surface almost separately when less plating solution is used. When more plating solution is used to plate the sample, the particles grow up and become irregular and connected to each other, therefore the fibers surface are coated with the coarse gold films finally. While there are more gold seeds in the hybrid fibers, the continuous smooth gold films are formed on the surface of the fibers.

The conductivities of the gold-coated mats have been measured by using the four-point probe method and the conductivities are found to be 3.0×10^2, 9.9×10^3 and 1.9×10^2 S cm^{-1} for 25S1, 25S2 and 3S2, respectively. And 3S1 is almost an insulator, revealing that the continuous gold films are not formed, which is consistent with that of SEM. The final gold-coated fibrous mats of 3S2 and 25S2 show a typical gold–yellow reflective surface.

In the XRD patterns (Fig. 3), the diffraction peak at about 17° is corresponding to the PAN (1 1 0) (Fig. 3a), and the four obvious diffraction peaks located at 38.21°, 44.45°, 64.68° and 77.65° are corresponding to the (1 1 1), (2 0 0), (2 2 0), and (3 1 1) planes of a face-centered cubic lattice of Au (PDF 4-784) (Fig. 3b and c). The peak corresponding to the (1 1 1) plane is more intense than that corresponding to the other planes. And the ratio between the intensities of (2 0 0) and (1 1 1) diffraction peaks is much lower than the conventional value, demonstrating that the (1 1 1) plane is the predominant orientation in 3S2 and 25S2 [42].

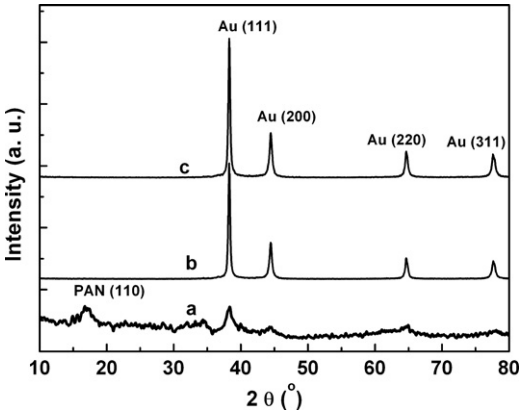

Fig. 3. The XRD patterns of (a) PAN/GNPs hybrid fibrous mat prepared from PAN/gold salt containing 25% (w/w) gold salt, (b) 3S2 and (c) 25S2.

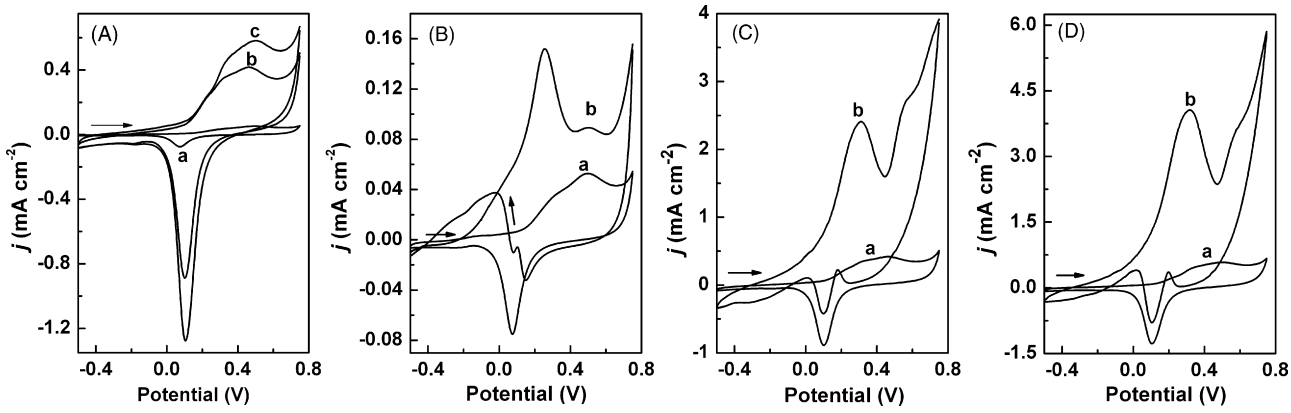

Fig. 4. Cyclic voltammograms of different gold electrodes. (A)—(a) pure gold, (b) 3S2 and (c) 25S2 in 0.1 mol l^{-1} KOH solution. (B–D)—(a) Pure gold, 3S2 and 25S2 electrode in 0.1 mol l^{-1} KOH solution, respectively; (b) pure gold, 3S2 and 25S2 electrode in 0.1 mol l^{-1} KOH + 2.0 mol l^{-1} methanol aqueous solution, respectively. The potential scan rate: 10 mV s^{-1}.

3.2. Electrocatalytic properties of the fibrous mats electrode for methanol

Fig. 4A shows the cyclic voltammograms obtained from the pure gold, 3S2 and 25S2 electrodes in 0.1 mol l^{-1} KOH aqueous solution. A broad oxidation wave located at about 0.50 V and a reduction wave located at 0.10 V, corresponding to the formation of gold surface oxides and their reductions are observed [43,44]. From Fig. 4A, we can also find that the peak current density of the mat electrodes is larger than that of pure gold electrode, revealing that there is high surface area in the mat electrodes because of the three-dimensional structure of the fibrous mats. Furthermore, the peak current density of 25S2 is larger than that of 3S2 because of the smaller gold particles in 25S2. The consumed charge during the reduction of gold oxides has been estimated by integrating the area under the reduction wave. According to the literature [45], by using the date of 400 μC cm^{-2} for a clean planar gold electrode, the actual surface areas of gold of the electrodes are calculated to be 1.9, 12.2 and 19.8 cm^2 per 1 cm^2 of geometric surface area for pure gold, 3S2 and 25S2 electrode, respectively.

The typical cyclic voltammograms obtained from oxidation of methanol on gold electrodes and mats electrodes are shown in Fig. 4B–D. For the pure gold electrode, the large anodic current peak at about 0.26 V observed in the presence of methanol come from the methanol oxidation, and the weak current peak at about 0.51 V is corresponding to the gold oxide formation, and after the potential of gold oxide formation the anodic current increase dramatically again. Such a characteristic voltammetric response in presence of methanol is also observed on the gold mats electrodes, the peak potential at about 0.31 V is assigned to the electrocatalytic oxidation of methanol, and after the potential of gold oxides formation the anodic current increases dramatically also again. According to the literature [46], we know that methanol is oxidized on gold electrodes in two potential regions, one is before gold oxide formation (first region) and the other is after the potentials corresponding to gold oxides formation (second region). The results in this paper are similar to that of previous reports.

From Fig. 4B–D, we can also find that the peak current density for methanol oxidation in the first region on the mats electrodes of 3S2 and 25S2 is about 15.4 and 26.3 times of that on pure gold electrode in term of geometric surface area, respectively. Furthermore, the peak current density of 25S2 is about 1.7 times of that of 3S2. Considering that the actual surface area of 25S2 electrode is about 10 and 1.6 times of that of pure gold and 3S2 electrode, the catalytic activity of 25S2 electrodes is 2.6 and 1.06 times of pure gold and 3S2 electrodes. The actual surface area of 3S2 is about 6.4 times of that of pure gold electrode, the catalytical activity of 3S2 electrode is 2.4 times of pure gold electrode.

At potential scan rates of 1–50 mV s^{-1}, the voltammetric responses of 25S2 electrode towards methanol oxidation have also been recorded (Fig. 5A). The smaller the potential scan rate the higher oxidation current in negatively-going scan is observed. With the increase of scan rate, the oxidation current increases and the peak potential shifts to more positive potential in the positively going scan, and the reduction current for gold oxide appears and increase in the negatively going scan at the same time. When the potential scan rate is small than 7 mV s^{-1}, the reduction current for gold oxides is very small in the negative potential scan, revealing that the gold oxide formation is inhibited. The anodic peak current density for methanol oxidation in the first region is approximately linear with $v^{1/2}$ at the scan rates of 1–7 mV s^{-1} with a large slope. However, at the scan rates of 10–50 mV s^{-1}, the peak current density for methanol oxidation in the first region is linear with $v^{1/2}$ with a small slope (Fig. 5B). The electrocatalytic activity of metallized fibrous mats is very stable against repetitive cycling in the potential window used, indicating that these electrodes are free from the poisoning effect [34,43].

The cyclic voltammograms recorded at different concentrations of methanol are shown in Fig. 6A, with the increase of the methanol content the anodic current for methanol oxidation increases, and the cathodic current for the gold oxides reduction decreases, revealing that the formation of surface gold oxides is inhibited by high concentration methanol in positively going scan. Fig. 6B shows the voltammograms recorded with different positive potential limit in

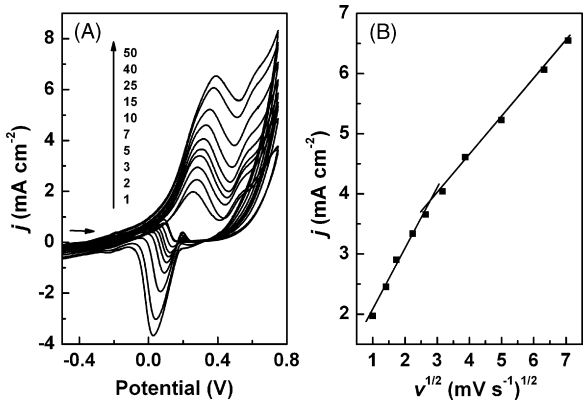

Fig. 5. (A) Cyclic voltammograms of 25S2 electrode at potential scan rate of 1–50 mV s^{-1} in 0.1 mol l^{-1} KOH + 2.0 mol l^{-1} methanol aqueous solution and (B) the plots of peak current density versus the $v^{1/2}$ for (A).

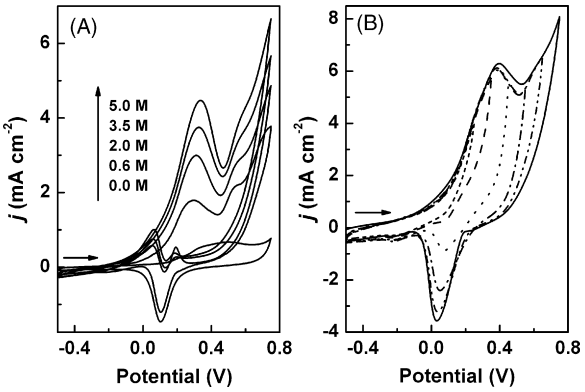

Fig. 6. (A) Cyclic voltammograms for the electro-oxidation of methanol on 25S2 electrode in 0.1 mol l^{-1} KOH at a scan rate 5 mV s^{-1}. Methanol concentrations are given in the figure and (B) cycling voltammograms for the electro-oxidation of 2.0 mol l^{-1} methanol solution in 0.1 mol l^{-1} KOH on 25S2 with different positive potential limits. Potential scan rate: 50 mV s^{-1}.

alkaline solution. With the decrease of the positive potential limit, the cathodic currents for gold oxide reduction decrease, while the anodic current for methanol oxidation is almost invariable when the potential limit is not less than the current peak potential. This fact also proves that in positively going potential scanning, the current peak for methanol oxidation is prior to the potential of gold oxide formation, and then this process is hindered by surface gold oxide formation and the amount of gold oxide increases with the increase of the positive potential.

In order to investigate electrocatalytic activities of pure gold electrode and the mat electrodes, the exchange current density (j_0) for methanol oxidation are calculated. The polarization studies for the pure gold and mats electrodes have been carried out, and the Tafel curves are shown in Fig. 7. According to the Tafel equation [47]:

$$\eta = \alpha - b\log j, \quad a = \frac{2.303RT\log j_0}{\alpha nF}, \quad b = \frac{2.303RT}{\alpha nF}$$

where $\eta = E - E_{eq}$ is named as the overpotential. Then, j_0 can be calculated according to the relationship of η and $\log j$. The values of j_0 are calculated with the same procedure to be 15.0 μA cm^{-2} on pure gold electrode, 34.7 μA cm^{-2} on 3S2 electrode and 40.5 μA cm^{-2} on 25S2 electrode. The j_0 value on 25S2 electrode is about 1.17 and 2.70 times as large as that on 3S2 and pure gold electrode, respectively. These indicate further that the smooth gold films formed by smaller particles deposited on the mats accelerate significantly the process

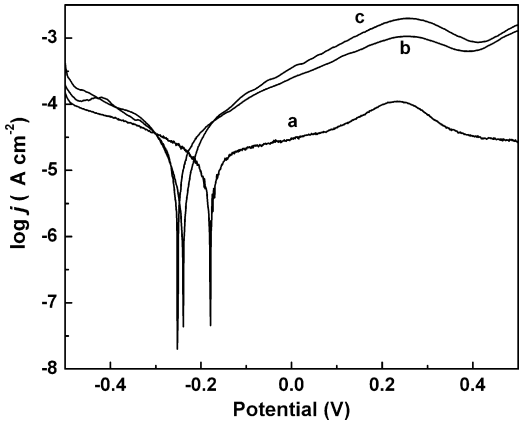

Fig. 7. Tafel plot of the different gold electrodes in 0.1 mol l^{-1} KOH + 2.0 mol l^{-1} CH_3OH at a potential scan rate of 1 mV s^{-1}: (a) Pure gold, (b) 3S2 and (c) 25S2 electrode.

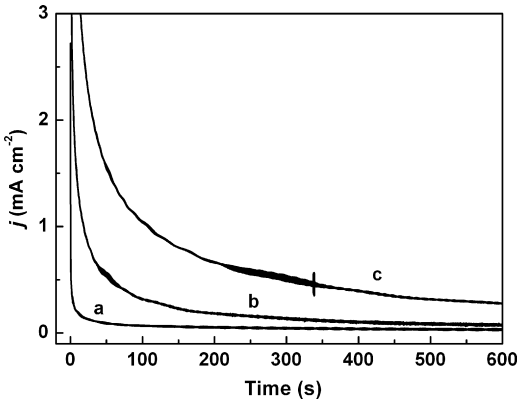

Fig. 8. Chronoamperometric plots for methanol oxidation on pure gold electrode (a), 3S2 electrode (b) and 25S2 electrode (c) recorded at potential of 0.25 V in 0.1 mol l^{-1} KOH + 2.0 mol l^{-1} CH_3OH aqueous solution.

of methanol electro-oxidation. On the other hand, the equilibrium potential also decreases obviously from −0.18 V at gold electrode to about −0.24 V at mat electrodes, which implies that methanol oxidation on the mats electrodes is easier than that on the pure gold electrode. The slopes of the Tafel curve are also calculated to be 293, 357 and 655 mV/decade on 25S2, 3S2 and pure gold electrode, indicating that 25S2 electrode has higher catalytical ability for methanol oxidation.

In practical application, the long-term stability of the electrode is of great importance. The stabilities of the pure gold electrode and mat electrodes have also been characterized by chronoamperometric method in 2.0 mol l^{-1} CH_3OH + 0.1 mol l^{-1} KOH aqueous solution at potential of 0.25 V. From Fig. 8, it can be observed obviously that the current density on the 25S2 electrode is higher than that on the pure gold electrode and 3S2 electrode, which is in accordance with the results shown in Fig. 4, denoting a strong catalytic behavior towards methanol oxidation at 25S2 electrode.

4. Conclusions

The continuous thin gold films formed by gold particles have been deposited on the surface of PAN ultrafine fibers prepared by electrospinning technique. The morphology of the resulted gold films is influenced by the amount of the gold seeds embedded in the fibers, and the smooth gold films tend to form on the surface of the fibers containing more gold seeds. The fibrous mats covered with smooth gold films have higher conductivities and higher electrocatalytic activity and can be directly used as electrode towards methanol oxidation due to the high available surface area of gold nanoparticles in three-dimensional structure of the metallized fibrous mat.

Acknowledgements

Financial support from National Natural Science Foundation of China with grant number of 20604014, Science Foundation of Shaxi Province with grant number of 2007021008, and Foundation for Young Scholar of Shanxi Province and Shanxi University.

References

[1] C. Burda, X.B. Chen, R. Narayanan, M.A. El-Sayed, Chem. Rev. 105 (2005) 1025.
[2] N.L. Rosi, C.A. Mirkin, Chem. Rev. 105 (2005) 1547.
[3] B. Yoon, H. Hakkinen, U. Landman, A.S. Worz, J.M. Antonietti, S. Abbet, K. Judai, U. Heiz, Science 307 (2005) 403.
[4] M. Date, M. Okumura, S. Tsubota, M. Haruta, Angew. Chem., Int. Ed. 43 (2004) 2129.
[5] S.Y. Lin, S.W. Liu, C.M. Lin, C.H. Chen, Anal. Chem. 74 (2002) 330.
[6] Y.J. Kim, R.C. Johnson, J.T. Hupp, Nano Lett. 1 (2001) 165.

[7] J.W. Liu, Y. Lu, Angew. Chem., Int. Ed. 45 (2006) 90.
[8] C. Loo, A. Lowery, N. Halas, J. West, R. Drezek, Nano Lett. 5 (2005) 709.
[9] W.L. Barnes, A. Dereux, T.W. Ebbesen, Nature 424 (2003) 824.
[10] Y.G. Sun, Y.N. Xia, Adv. Mater. 14 (2002) 833.
[11] J. Guzman, B.C. Gates, J. Am. Chem. Soc. 126 (2004) 2672.
[12] Y.D. Jin, X.F. Kang, Y.H. Song, B.L. Zhang, G.J. Cheng, S.J. Dong, Anal. Chem. 73 (2001) 2843.
[13] B. Ren, G. Picardi, B. Pettinger, R. Schuster, G. Ertl, Angew. Chem., Int. Ed. 44 (2005) 139.
[14] H. Wang, C.S. Levin, N.J. Halas, J. Am. Chem. Soc. 127 (2005) 14992.
[15] L. Lu, I. Randjelovic, R. Capek, N. Gaponik, J. Yang, H. Zhang, A. Eychmueller, Chem. Mater. 17 (2005) 5731.
[16] L. Supriya, R.O. Claus, Langmuir 20 (2004) 8870.
[17] S. Hrapovic, Y.L. Liu, G. Enright, F. Bensebaa, J.H.T. Luong, Langmuir 19 (2003) 3958.
[18] K.R. Brown, M.J. Natan, Langmuir 14 (1998) 726.
[19] C.A. Goss, D.H. Charych, M. Majda, Anal. Chem. 63 (1991) 85.
[20] G.Y. Han, G.Q. Shi, J. Appl. Polym. Sci. 103 (2007) 1490.
[21] M.S. Khil, H.Y. Kim, M.S. Kim, S.Y. Park, D.R. Lee, Polymer 45 (2004) 295.
[22] J.R. Kim, S.W. Choi, S.M. Jo, W.S. Lee, B.C. Kim, Electrochim. Acta 50 (2004) 69.
[23] S. Madhugiri, A. Dalton, J. Gutierrez, J.P. Ferraris, K.J. Balkus Jr., J. Am. Chem. Soc. 125 (2003) 14531.
[24] L. Yao, T.W. Haas, A. Guiseppi-Elie, G.L. Bowlin, D.G. Simpson, G.E. Wnek, Chem. Mater. 15 (2003) 1860.
[25] G. Larsen, R. Velarde-Ortiz, K. Minchow, A. Barrero, I.G. Loscertales, J. Am. Chem. Soc. 125 (2003) 1154.
[26] H.Q. Hou, D.H. Reneker, Adv. Mater. 16 (2004) 69.
[27] F. Ko, Y. Gogotsi, A. Ali, N. Naguib, H. Ye, G. Yang, C. Li, P. Wills, Adv. Mater. 15 (2003) 1161.
[28] Z.M. Huang, Y.Z. Zhang, M. Kotaki, S. Ramkrishna, Compos. Sci. Technol. 63 (2003) 2223.
[29] D. Li, Y.N. Xia, Adv. Mater. 16 (2004) 1151.
[30] G.Y. Han, B. Guo, L.W. Zhang, B.S. Yang, Adv. Mater. 18 (2006) 1709.
[31] M. Bognitzki, M. Becker, M. Graeser, W. Massa, J.H. Wendorff, A. Schaper, D. Weber, A. Beyer, A. Goelzhaeuser, Adv. Mater. 18 (2006) 2384.
[32] F. Ochanda, W.E. Jones, Langmuir 21 (2005) 10791.
[33] F. Ochanda, W.E. Jones, Langmuir 23 (2007) 795.
[34] Y.B. Lou, M.M. Maye, L. Han, J. Luo, C.J. Zhong, Chem. Commun. (2001) 473.
[35] L. Yang, J.H. Chen, X.X. Zhong, K.Z. Cui, Y. Xu, Y.F. Kuang, Colloids Surf. A 295 (2007) 21.
[36] V. Georgakilas, D. Gournis, V. Tzitzios, L. Pasquato, D.M. Guldi, M. Prato, J. Mater. Chem. 17 (2007) 2679.
[37] Y.H. Chu, S.W. Ahn, D.Y. Kim, H.J. Kim, Y.G. Shul, H. Han, Catal. Today 111 (2006) 176.
[38] H.O. Finklea, S. Avery, M. Lynch, Langmuir 3 (1987) 409.
[39] B.K. Jena, C.R. Raj, Chem. Eur. J. 12 (2006) 2702.
[40] H.-J. Kim, D.-Y. Kim, H. Han, Y.-G. Shul, J. Power Sources 159 (2006) 484.
[41] K. Miyazaki, H. Ishihara, K. Matsuoka, Y. Iriyama, K. Kikuchi, Y. Uchimoto, T. Abe, Z. Ogumi, Electrochim. Acta 52 (2007) 3582.
[42] Z.Z. Hou, N.L. Abbott, P. Stroeve, Langmuir 14 (1998) 3287.
[43] B.K. Jena, C.R. Raj, Langmuir 23 (2007) 4064.
[44] J. Luo, M.M. Maye, Y. Lou, L. Han, M. Hepel, C.J. Zhong, Catal. Today 77 (2002) 127.
[45] H. Angerstein-Kozlowska, B.E. Conway, A. Hamelin, L. Stoicoviciu, J. Electroanal. Chem. 228 (1987) 429.
[46] Z. Borkowska, A. Tymosiak-Zielinska, G. Shul, Electrochim. Acta 49 (2004) 1209.
[47] D.W. Pan, J.H. Chen, W.Y. Tao, L.H. Nie, S.Z. Yao, Langmuir 22 (2006) 5872.